Intra-myocardial Delivery of Mesenchymal Stem Cells Ameliorates Left Ventricular and Cardiomyocyte Contractile Dysfunction Following Myocardial Infarction

Qun Li[1,*], **Subat Turdi**[1,*], **D. Paul Thomas**[2], **Tianjie Zhou**[3], and **Jun Ren**[1]

[1]Division of Pharmaceutical Sciences & Center for Cardiovascular Research and Alternative Medicine, University of Wyoming, Laramie, WY 82071, USA

[2]Division of Kinesiology & Health, University of Wyoming, Laramie, WY 82071, USA

[3]Laramie High School, Laramie, WY 82071

Abstract

Although mesenchymal stem cells (MSC) transplantation may improve the overall heart function, the heterogeneity of myocardial cells makes it difficult to determine the nature of cells benefited from transplantation. This study evaluated the effect of intra-myocardial MSC transplantation on myocardial function following MI. Enhanced green fluorescent protein (EGFP)-expressing donor MSCs from C57BL/6-Tg (UBC-GFP) 30Scha/J mice were transplanted into LV free wall in the region bordering an infarct in C57 recipient mice following ligation of left main coronary artery (MI +MSC group). Ten days after MI, LV function was assessed using echocardiography. Cardiomyocyte contractility and intracellular Ca^{2+} transients were measured in cells from the area at risk surrounding the infarct scar. The EGFP donor cells were traced in the MSC recipient mice using fluorescence microscopy. TUNEL, H&E and Masson trichrome staining were used to assess apoptosis, angiogenesis and myocardial fibrosis, respectively. MI dilated LV as evidenced by increased end-diastolic and systolic diameters. MI significantly reduced fractional shortening, cardiomyocyte peak shortening, and maximal velocity of shortening and relengthening, all of which were attenuated or abrogated by MSC therapy. MI also reduced resting intracellular Ca^{2+}, intracellular Ca^{2+} rise and decay rate, which were reconciled by MSC. MSC therapy attenuated MI-induced apoptosis and decreased angiogenesis but not myocardial fibrosis in peri-infarct area. Taken together, our results demonstrated that MSC therapy significantly improved both LV and cardiomyocyte function possibly associated with its beneficial role in apoptosis and angiogenesis, indicating a key role for cardiomyocytes in stem cell tissue engineering.

Keywords

Myocardial infarction; Mesenchymal stem cell; Contraction; Intracellular Ca^{2+} transients; Apoptosis; Angiogenesis

Publisher's Disclaimer: This is a PDF file of an unedited manuscript that has been accepted for publication. As a service to our customers we are providing this early version of the manuscript. The manuscript will undergo copyediting, typesetting, and review of the resulting proof before it is published in its final citable form. Please note that during the production process errors may be discovered which could affect the content, and all legal disclaimers that apply to the journal pertain.

INTRODUCTION

Cardiovascular diseases remain the leading cause of death in industrialized countries with ischemic heart diseases contributing to ~40% of the entire cardiovascular morbidity. When primary and secondary prevention fail and myocardial infarction (MI) ensues, myocardial tissues are subject to irreversible necrosis. Given the high prevalence of cardiac morbidity and mortality in patients with MI, interventional strategies are under intense scrutiny for better management of MI. Among all maneuvers for post-MI treatment, one of the recent promising approaches is the myocardial cell transplantation which involves implantation of muscle cells, progenitor cells and pluripotent stem cells into the infarct region. Accumulating evidence indicates that transplantation of adult stem cells derived from bone marrow may exert a beneficial effect on the overall cardiac function (Piao et al. 2005; Grauss et al. 2007; Wang et al. 2008). Makino and colleagues reported that bone marrow (BM)-derived mesenchymal stem cells (MSC) may be differentiated into the spontaneously beating cardiomyocytes *in vitro* (Hakuno et al. 2002; Makino et al. 1999; Tomita et al. 2007). Similarly, *in vivo* evidence has been obtained with regards to the amendment of injured myocardium using MSC transplantation (Toma et al. 2002; Tomita et al. 1999). Following their introduction into the infarct heart, bone marrow cells are capable of alleviating deleterious remodeling and facilitating tissue recovery. Although MSC transplantation is believed to improve the overall myocardial pump function, the nature of the heterogeneity of cells within myocardium makes it rather difficult to discern the precise cell types benefited from the transplantation procedure. Therefore, it is essential to monitor single cell contractile function in order to assess the role of the basic contractile element in the heart, namely cardiomyocytes. In this study, enhanced green fluorescent protein (EGFP)-expressing donor MSCs were transplanted into recipient hearts immediately following ligation of left coronary artery. Ten days following transplantation, fraction shortening, LV end diastolic and LV end systolic diameters were evaluated in post-MI murine hearts with or without MSC transplantation. Moreover, individual cardiomyocyte contractile and intracellular Ca^{2+} properties were evaluated in cells from the area at risk. The fate of the MSC donor cells was traced using the fluorescent microscopy. Given that stem cell-based tissue engineering may achieve its beneficial effect through production of tissue factors counteracting apoptosis or promoting angiogenesis in addition to direct cell regenerative action (Martin et al. 2010; Berry et al. 2006), histopathological examination was performed to evaluate apoptosis, angiogenesis and myocardial fibrosis in post-MI hearts with or without MSC transplantation.

MATERIALS AND METHODS

GFP mice and culture of bone marrow mesenchymal stem cells (MSCs)

The experimental procedure described in this study was approved by our Institutional Animal Use and Care Committee and was in compliance with the Guide for the Care and Use of Laboratory Animals published by the US National Institutes of Health (NIH Publication No. 85-23, revised 1996). In brief, the EGFP transgenic mice with overexpression of GFP (on C57BL/6J background) were purchased from Jackson laboratory. Four to six months C57BL/6J mice were used as the stem cell recipient or control mice. All mice were housed in a temperature-controlled room under a 12hr/12hr-light/dark and allowed access to tap water *ad libitum*. Four to six week-old GFP mice were anesthetized with ketamine/xylazine (3:1, 1.32 mg/kg, i.p.). The bone-marrow plugs of the femora and tibiae were flushed using a 22-gauge needle and a syringe filled with phosphate-buffered saline solution (PBS). Bone-marrow cells were suspended in a tube containing PBS and centrifuged at 1,000×g for 5 min. Cell pellets were then resuspended in a MesenCultTM medium supplemented with Mesenchymal Stem cell Stimulatory Supplements (StemCell Technologies. Vancouver, Canada) and were incubated in 37°C with 5% CO_2. The primary cultures of MSC were able to reach ~90%

confluence in 10 days. The third-to-fifth passage cells were trypsinized and suspended in PBS before being used for transplantation purpose (Toma et al. 2002; Anjos-Afonso et al. 2004).

Myocardial infarction model and cell transplantation

Adult male C57BL/6J mice (4–6 month-old) were endotracheally intubated and ventilated using a rodent ventilator. Anesthesia was maintained with a ketamine/xylazine anesthetic/ analgesic combination. Thoracotomy was performed and a 6-0 ethilon ligature was placed around the left anterior descending artery 4–5 mm above the left atrium. Approximately 5×10^5 MSCs were injected into non-ischemic (border) zones (single injection). Then the chest was then closed before the animals were weaned from the ventilator and were extubated. Occlusion of the left anterior descending coronary artery and injection of MSCs were performed surgically with the aid of a Leica dissecting microscope. Border zones were chosen for MSC transplantation primarily to maximize graft viability. The ischemic and proapoptotic nature of the infarcted region is deemed unsuitable for graft viability. Mice were maintained on a Harvard small animal respirator during the thoracotomy, infarct, injection and recovery procedures (McCormick et al. 1994).

Echocardiographic assessment

In vivo cardiac contractile function was studied using a Sonos 5500 echocardiography unit (Hewlett-Packard, Andover, MA) as described (Doser et al. 2009). Mice were sedated and normothermia was maintained with a heating pad. A 15-6 mHz linear array pediatric probe was placed in the parasternal, short axis orientation to record LV systolic and diastolic internal dimensions. Three loops of M-mode data were captured for each animal, and data are averaged from at least 5 beat cycles per loop. Parameters were determined using the American Society for Echocardiography leading-edge technique in a blinded fashion. The measurements included those of LV chamber diameter in systole and diastole as well as fractional shortening as an index of left ventricular systolic performance. Fractional shortening was calculated from LV end-diastolic (LVEDD) and end-systolic (LVESD) diameters using the equation (LVEDD-LVESD)/LVEDD.

Preparation of cryostat section from heart tissue after stem cell transplantation

To track the fate of stem cells, ten days after transplantation, cryostat sections were cut from snap-frozen heart tissues around the site of stem cell injection. Tissue section thickness was 5 µm.

Isolation of mouse ventricular myocytes

Mouse hearts were removed under anesthesia (ketamine/xylazine at 3:1, 1.32 mg/kg) and were perfused with Krebs-Henseleit bicarbonate buffer containing (in mM): 118 NaCl, 4.7 KCl, 1.2 $MgSO_4$, 1.2 KH_2PO_4, 25 $NaHCO_3$, 10 HEPES, 11.1 glucose and 10 butanedione with 5% CO_2-95% O_2. Hearts were subsequently digested with 0.1mg/ml Liberase Blendzymes (Roche Diagnostics, Indianapolis, IN, USA) for around 10 min at 37°C. After perfusion, border zone of ventricles and area at risk were removed and minced respectively. Cells from border zone were used to locate the GFP-positive cells under fluorescence. Extracellular Ca^{2+} was added back to 1.25 mM to cells of area at risk. Functional studies were conducted between 1 and 8 hrs of isolation and myocytes with obvious sarcolemmal blebs or spontaneous contractions were not used for study (Doser et al. 2009).

Cell shortening/relengthening

Mechanical properties of ventricular myocytes were assessed using a SoftEdge MyoCam® system (IonOptix Corporation, Milton, MA, USA) (Doser et al. 2009). In brief, left ventricular myocytes were placed in a chamber mounted on the stage of an inverted microscope (Olympus

Incorporation, Model IX-70, Tokyo, Japan) and superfused at 25°C with a buffer containing (in mM): 131 NaCl, 4 KCl, 1 $CaCl_2$, 1 $MgCl_2$, 10 glucose, 10 HEPES, at pH 7.4. The cells were field stimulated with suprathreshold voltage at a frequency of 0.5 Hz (unless otherwise stated), 3 msec duration, using a pair of platinum wires placed on opposite sides of the chamber connected to a FHC stimulator (Brunswick, NE, USA). The myocyte being studied was displayed on a computer monitor using an IonOptix MyoCam camera. An IonOptix SoftEdge software was used to capture changes in cell length during shortening and relengthening. In the case of altering stimulus frequency from 0.1 to 5.0 Hz, the steady state contraction of myocyte was achieved (usually after the first 5–6 beats) before PS was recorded (Li and Ren 2006).

Intracellular Ca^{2+} transient measurement

Intracellular Ca^{2+} was measured using a dual-excitation, single-emission photomultiplier system (IonOptix) in myocytes loaded with fura-2-AM (0.5 µM). Myocytes were placed on an inverted microscope and imaged through an Olympus (IX-70) Fluor ×40 oil objective. Myocytes were exposed to light emitted by a 75-W halogen lamp through either a 360- or 380-nm filter while being stimulated to contract at 0.5 Hz. Fluorescence emissions were detected between 480 and 520 nm by a photomultiplier tube after initial illumination at 360 nm for 0.5 s and then at 380 nm for the duration of the recording protocol. The 360-nm excitation reading was repeated at the end of the protocol. Qualitative evaluation of intracellular Ca^{2+} was inferred from fura-2 fluorescence intensity (FFI) changes (ΔFFI). A Chebyshev equation was used to evaluate the single- and bi-exponential intracellular Ca^{2+} decay constant (Yang et al. 2006).

TUNEL assessment of apoptosis

TUNEL (terminal deoxynucleotidyl transferase-mediated dUTP nick-end labeling) staining of myonuclei positive for DNA strand breaks was determined using a fluorescence detection kit (Roche Applied Science Indianapolis, IN) and fluorescence microscopy. Ten days after MSC injection, the hearts were transversely cut in mid-level. Cross sections (5 µm) of hearts with a Leica cryostat were fixed in 4% paraformaldehyde for 20 min and then fixed sections were permeabilized with 0.1% Triton X-100 in 0.1% sodium citrate for 2 min on ice. TUNEL reaction mixture containing terminal deoxynucleotidyl transferase (TdT), fluorescein-dUTP was added to the sections in 50-µl drops and incubated for 60 min at 37°C in a humidified chamber in the dark. The sections were rinsed three times in PBS for 5 min each. Following embedding, sections were visualized with an Olympus BX-51 microscope equipped with an Olympus MaguaFire SP digital camera. DNase I and label solution were used as positive and negative controls. To determine the percentage of apoptotic cells, micrographs of TUNEL-positive nuclei and DAPI-stained nuclei were captured using an Olympus fluorescence microscope and counted using the ImageJ software (ImageJ version 1.43r; NIH) from 21–30 random fields at 400 × magnification (Ren et al. 2009).

H&E staining and angiogenesis

Following anesthesia, hearts were excised and immediately placed in 10% neutral-buffered formalin at room temperature for 24 hrs after a brief rinse with PBS. The heart specimen were embedded in paraffin, cut in 5 µm sections and stained with hematoxylin and eosin (H&E). Vascular density analysis was then performed on H&E stained sections. In brief, 4 high-power fields (400 × magnification) in each section were randomly selected in the peri-infarct area, the number of capillaries in each field was counted and shown as the number of capillary vessels per unit area (0.14 mm^2). Furthermore, myocardial section were stained with Masson trachoma and fibrosis area in the peri-infarct area was calculated from 10–15 random fields (400 × magnifications) by dividing the pixels of blue stained area to the total pixels of non-white area in per section using Photoshop (Nishiya et al. 2006; Tang et al. 2006).

Statistical analysis

Data were Mean ± SEM. Statistical significance ($p < 0.05$) for all other variables was determined by one-way analysis of variance followed by a Tukey's *post hoc* test.

RESULTS

Echocardiographic assessment

Ten days following MI and stem cell transplantation, the *in vivo* LV contractile function and geometry were evaluated using echocardiographic technique. Echocardiographic indices included LV chamber diameter (both systole and diastole) and fractional shortening as an index of left ventricular performance. Our data shows that MI significantly reduced fraction shortening and increased LV diameters (both end diastolic and end systolic). Stem cell transplantation significantly attenuated (fractional shortening and LVESD) or ablated (LVEDD) the MI-induced changes in LV performance and geometry (Fig. 1).

Verification of stem cells in tissue slides and isolated cardiomyocyte from border zone

To trace the fate of stem cells transplanted to the border zone 10 days following MI, slides from myocardium were made by every 15 µm of tissues away from the border zone. All sections were placed under microscopy to locate the GFP-positive cells. Fig. 2A and Fig. 2B display a few GFP-positive cells found in the border zone. Meanwhile, the GFP-positive cardiomyocytes were also found in the isolated cells from border zone (Fig. 2C and Fig. 2D).

Baseline mechanical and intracellular Ca^{2+} properties of left ventricular cardiomyocytes

Data shown in Fig. 3 indicate that MI significantly reduced peak shortening (PS) amplitude, maximal velocity of shortening/relengthening ($\pm$ dL/dt) without affecting time-to-PS (TPS) and time-to-90% relengthening (TR_{90}) in cells from area-at-risk in C57 mice. Interestedly, transplantation of MSCs significantly attenuated or abrogated the MI-induced mechanical dysfunctions while shortening TR_{90} by itself. To explore the possible role of intracellular Ca^{2+} homeostasis in MI- and MSC transplantation-induced mechanical responses, intracellular Ca^{2+} transients were assessed in cells from the area-at-risk using fura-2 fluorescence. Our result indicated that MI reduced resting and electrically-induced rise of intracellular Ca^{2+} levels as well as prolonged intracellular Ca^{2+} clearing (single and bi-exponential decay rate), all of which were significantly attenuated or nullified by MSC transplantation (Fig. 4).

Effect of increasing stimulation frequency on myocyte shortening

Rodent hearts normally contract at high frequencies, whereas our mechanical recording was performed at 0.5 Hz. To evaluate the impact of MI with or without MSC transplantation on cardiac contractile function under higher frequency, we increased stimulus frequency up to 5.0 Hz (300 beats/min) and recorded the steady-state peak shortening. Cardiomyocytes were initially stimulated to contract at 0.5 Hz for 5 min to ensure a steady-state before commencing the frequency response. Fig. 5 displays a negative staircase in PS with increased stimulus frequency in all 3 groups with a steeper decline in MI group compared with the control (PS was normalized to its value at 0.1 Hz of the same myocyte). MSC transplantation effectively cancelled off the MI-induced decline in PS at higher (3 and 5 Hz) but not at lower (0.5 and 1 Hz) stimulus frequencies. These data favor a possible role of reduced intracellular Ca^{2+} cycling or stress tolerance capacity underscoring MI-associated cardiomyocyte mechanical defect, which may be reconciled by MSC transplantation at higher stimulus frequencies.

Histological examination

Given that MSC transplantation may decrease apoptosis, promote angiogenesis and affect myocardial fibrosis in the peri-infarct area (Berry et al. 2006; Martin et al. 2010),

histopathological examination was performed to evaluate apoptosis, angiogenesis and myocardial fibrosis in post-MI hearts with or without MSC transplantation. TUNEL staining data revealed that MI significantly enhanced myocardial apoptosis, the effect of which was attenuated by MSC transplantation (Fig. 6). Furthermore, H&E and Mason Trichrome staining displayed overt loss of vessel content (vascular density) and myocardial fibrosis following MI. MSC transplantation significantly attenuated the MI-induced loss of vascular content (angiogenesis) without affecting myocardial fibrosis following MI (Fig. 7). These data suggest that MSC transplantation may indirectly benefit myocardial function through reduced apoptosis and/or facilitated angiogenesis in the post-infarct hearts.

DISCUSSION

Much effort has been made over the last decades towards novel therapeutic strategies for the management of cardiovascular disease, especially ischemic heart diseases. Stem cell transplantation has received some attention recently as a promising remedy against MI. Data from our current study demonstrated that MSCs transplantation can indeed restore MI-induced heart dysfunction. This result is consistent with the findings from previous reports (Piao et al. 2005; Grauss et al. 2007; Wang et al. 2008). Our salient finding is that MSC transplantation can significantly ameliorate or abrogate MI-induced echocardiographic, cardiomyocyte contractile and intracellular Ca^{2+} dysfunction. Although MSC transplantation may improve the overall heart function (Piao et al. 2005; Wang et al. 2008), our work revealed for the first time that the improved myocardial contractile function following MSC transplantation may be due to, at least in part, the beneficial effect of cell transplantation in individual cardiomyocytes from the area-at-risk. Nonetheless, the beneficial mechanical responses were coordinated with reduced apoptosis and facilitated angiogenesis but not fibrosis in post-MI myocardium following MSC treatment, indicating possible contributions of anti-apoptosis and angiogenesis in MSCs-exerted myocardial effect following MI.

One of the major adverse effects of MI in the hearts is the significantly reduced fraction shortening, which is in concert with increased LV end diastolic and end systolic diameters favoring dilation of LV chamber (Piao et al. 2005; Wang et al. 2008). This notion is supported by the findings from our present observation. Furthermore, our data revealed that all these anomalies were overtly attenuated or ablated by MSC transplantation. Using cardiomyocytes from the area-at-risk surrounding the infracted region, MI was found to significantly reduce peak shortening (PS) amplitude, and maximal velocity of shortening/relengthening ($\pm$ dL/dt) without affecting duration of contraction and relaxation. Interestingly, transplantation of MSCs ameliorated these abnormalities and also significantly shortened the diastolic duration TR_{90}. Our result further indicated that MI reduced resting and rise of intracellular Ca^{2+} levels as well as prolonged intracellular Ca^{2+} clearing. Consistent with the data from mechanical assessment, all of the MI-triggered intracellular Ca^{2+} handling defects were nullified by the MSC transplantation. The fact that MSC transplantation ameliorated MI-associated steeper decline in PS amplitude in response to high stimulus frequencies further consolidated the pivotal role of intracellular Ca^{2+} cycling in MI-induced cardiac mechanical defect and the therapeutic benefit of MSC transplantation. It is unclear at this point why MSC transplantation failed to affect the loss in PS amplitude at low stimulus frequencies (0.5 and 1 Hz) in post-MI murine cardiomyocytes. It may be speculated that discrepant effects on various intracellular Ca^{2+} cycling proteins (e.g., the rapid Ca^{2+} cycling by SERCA and the slow Ca^{2+} extrusion by Na^+-Ca^{2+} exchanger) may play a role.

Evidence from preclinical studies has shown that stem cells are capable of restoring the impaired cardiac function following MI including embryonic stem cells (Leor et al. 2007), bone marrow stromal cells (Iso et al. 2007), mesenchymal stem cells (Piao et al. 2005; Grauss et al. 2007; Wang et al. 2008), human cord blood cells (Ma et al. 2005), progenitor cells in

heart (Urbanek et al. 2005) and recently the human menstrual blood-derived mesenchymal cells (Hida et al. 2008). Although embryonic stem cells are totipotent cells (the ability of a single cell to divide and produce all the differentiated cells in an organism including extraembryonic tissues), the use of embryonic stem cells is rather limited due to apparent ethical issues. On the other hand, MSCs are a type of adult stem cells with promising therapeutic applications. Stem cells residing in hearts are usually named cardiac stem cells with a much higher potential to be differentiated into myocytes for amendment of the damaged heart. Nonetheless, cardiac stem cells are rare with an average of one cardiac stem cell per 18,000 cardiomyocytes (Linke et al. 2005; Urbanek et al. 2005). As a result, it is rather difficult to cultivate cardiac stem cells *in vitro*, which provides the rationale of selecting MSCs as a fairly good source for myocardial repair. MSC transplantation was found to improve the whole heart function following MI including fractional shortening (Imanishi et al. 2008), LVEF and LVEDV (Lu et al. 2008). Moreover, our present data revealed that MSC transplantation may reconcile left ventricular dilation and dysfunction indirectly via reduced cardiomyocyte apoptosis and increased vascular density (angiogenesis) but unlikely related to changes in myocardial fibrosis. Several rationales have been postulated for MSC transplantation-elicited beneficial myocardial anti-apoptotic and pro-angiogenic effects including inhibition of NF-κB activity, TNF-α and IL-6 production, as well as increased IL-10 expression (Du et al. 2008), plasma VEGF levels and capillary density (Imanishi et al. 2008).

The viability of implanted stem cells was shown to be low when injected directly to the infract region due to severe ischemic injury and apoptosis (Zhang et al. 2001). With this in mind, MSCs were delivered to the border area to maximally increase the cell viability. When the fate of MSCs was traced, only a few GFP-positive cells were found (approximately 1% to 2%) in the border zone from the recipient hearts (data not shown). Given the robust beneficial effect of intramyocardial MSC transplantation on echocardiographic, cardiomyocyte contractile and intracellular Ca^{2+} function, it is plausible to speculate that MSC transplantation may benefit myocardial function through reduced apoptosis and/or facilitated angiogenesis, in addition to its cell regenerative property, in the post-infarct hearts. It was reported that bone marrow-derived stem cells contribute only a small proportion of regenerated myocardium after MI (Fukuhara et al. 2005). Consistent with our current experimental findings, several alternate avenues have been recommended to improve the survival rate and differentiation of stem cell to combat with the myocyte loss following MI. In particular, facilitated angiogenesis through signaling molecules (e.g., VEGF), increased endothelial progenitor cell number using medical treatments (such as statins), transfection of stem cells with heat shock protein 70 (as a cardioprotective agent against ischemia) and enhanced stem cell survival with various forms of stimulating factors (G-CSF, SCF, GM-CSF) have all been suggested to produce favorable outcomes (Vertesaljai et al. 2008).

Experimental limitations: In our current experimental setting, only viable cardiomyocytes were taken for functional analysis which may have discounted the possible contribution from the difference in viable cardiomyocyte numbers among all experimental groups. This was largely hampered by certain technical factors such as the area of the "area-at-risk" and accurate quantification of viable cardiomyocytes. In addition, we did not perform immunosuppression in the recipient mice which is a common practice for cell transplantation procedure. Recent data from both human and other species have shown that MSCs possess a cell surface phenotype poorly immunogenic (Majumdar et al. 2003), thus leaving the application of immunosuppressant such as dexamethasone relatively less important in our current study.

In conclusion, data from our study indicated that MSC transplantation may improve the whole heart dysfunction following MI. Furthermore, MSC transplantation effectively ameliorates MI-induced cardiomyocyte contractile and intracellular Ca^{2+} dysfunction in cells from area-at-risk. Furthermore, MSC therapy significantly attenuated MI-induced apoptosis and decrease

in angiogenesis in the peri-infarct area. These results should have shed some light towards better understanding the stem cell therapy against ischemic heart diseases. In addition to the known neo-angiogenesis and regeneration of myocyte, other benefits that MSCs may provide such as on cardiomyocyte contractile function warrants further intensive study.

Acknowledgments

References

Anjos-Afonso F, Siapati EK, Bonnet D. In vivo contribution of murine mesenchymal stem cells into multiple cell-types under minimal damage conditions. J. Cell Sci 2004;117:5655–5664. [PubMed: 15494370]

Berry MF, Engler AJ, Woo YJ, Pirolli TJ, Bish LT, Jayasankar V, Morine KJ, Gardner TJ, Discher DE, Sweeney HL. Mesenchymal stem cell injection after myocardial infarction improves myocardial compliance. Am J Physiol Heart Circ Physiol 2006;290:H2196–H2203. [PubMed: 16473959]

Doser TA, Turdi S, Thomas DP, Epstein PN, Li SY, Ren J. Transgenic overexpression of aldehyde dehydrogenase-2 rescues chronic alcohol intake-induced myocardial hypertrophy and contractile dysfunction. Circulation 2009;119:1941–1949. [PubMed: 19332462]

Du YY, Zhou SH, Zhou T, Su H, Pan HW, Du WH, Liu B, Liu QM. Immuno-inflammatory regulation effect of mesenchymal stem cell transplantation in a rat model of myocardial infarction. Cytotherapy 2008;10:469–478. [PubMed: 18608353]

Fukuhara S, Tomita S, Nakatani T, Yutani C, Kitamura S. Endogenous bone-marrow-derived stem cells contribute only a small proportion of regenerated myocardium in the acute infarction model. J. Heart Lung Transplant 2005;24:67–72. [PubMed: 15653382]

Grauss RW, Winter EM, van TJ, Pijnappels DA, Steijn RV, Hogers B, van der Geest RJ, de Vries AA, Steendijk P, van der LA, Gittenberger-de Groot AC, Schalij MJ, Atsma DE. Mesenchymal stem cells from ischemic heart disease patients improve left ventricular function after acute myocardial infarction. Am. J. Physiol Heart Circ. Physiol 2007;293:H2438–H2447. [PubMed: 17644573]

Hakuno D, Fukuda K, Makino S, Konishi F, Tomita Y, Manabe T, Suzuki Y, Umezawa A, Ogawa S. Bone marrow-derived regenerated cardiomyocytes (CMG Cells) express functional adrenergic and muscarinic receptors. Circulation 2002;105:380–386. [PubMed: 11804996]

Hida N, Nishiyama N, Miyoshi S, Kira S, Segawa K, Uyama T, Mori T, Miyado K, Ikegami Y, Cui C, Kiyono T, Kyo S, Shimizu T, Okano T, Sakamoto M, Ogawa S, Umezawa A. Novel cardiac precursor-like cells from human menstrual blood-derived mesenchymal cells. Stem Cells 2008;26:1695–1704. [PubMed: 18420831]

Imanishi Y, Saito A, Komoda H, Kitagawa-Sakakida S, Miyagawa S, Kondoh H, Ichikawa H, Sawa Y. Allogenic mesenchymal stem cell transplantation has a therapeutic effect in acute myocardial infarction in rats. J. Mol. Cell Cardiol 2008;44:662–671. [PubMed: 18343403]

Iso Y, Spees JL, Serrano C, Bakondi B, Pochampally R, Song YH, Sobel BE, Delafontaine P, Prockop DJ. Multipotent human stromal cells improve cardiac function after myocardial infarction in mice without long-term engraftment. Biochem. Biophys. Res. Commun 2007;354:700–706. [PubMed: 17257581]

Leor J, Gerecht S, Cohen S, Miller L, Holbova R, Ziskind A, Shachar M, Feinberg MS, Guetta E, Itskovitz-Eldor J. Human embryonic stem cell transplantation to repair the infarcted myocardium. Heart 2007;93:1278–1284. [PubMed: 17566061]

Li Q, Ren J. Cardiac overexpression of metallothionein rescues chronic alcohol intake-induced cardiomyocyte dysfunction: role of Akt, mammalian target of rapamycin and ribosomal p70s6 kinase. Alcohol Alcohol 2006;41:585–592. [PubMed: 17020909]

Linke A, Muller P, Nurzynska D, Casarsa C, Torella D, Nascimbene A, Castaldo C, Cascapera S, Bohm M, Quaini F, Urbanek K, Leri A, Hintze TH, Kajstura J, Anversa P. Stem cells in the dog heart are self-renewing, clonogenic, and multipotent and regenerate infarcted myocardium, improving cardiac function. Proc. Natl. Acad. Sci. U. S. A 2005;102:8966–8971. [PubMed: 15951423]

Lu MJ, Zhao SH, Liu S, Zhang PH, Jiang SL, Zhang Y, Yan CW, Liu Q, Ling J, Huang LJ, He ZX, Yang MF, Hu SS. [Assessment of therapeutic effects of stem cell transplantation in heart failure patients with old myocardial infarction by magnetic resonance imaging]. Zhonghua Xin. Xue. Guan. Bing. Za Zhi 2008;36:969–974. [PubMed: 19102907]

Ma N, Stamm C, Kaminski A, Li W, Kleine HD, Muller-Hilke B, Zhang L, Ladilov Y, Egger D, Steinhoff G. Human cord blood cells induce angiogenesis following myocardial infarction in NOD/scid-mice. Cardiovasc. Res 2005;66:45–54. [PubMed: 15769447]

Majumdar MK, Keane-Moore M, Buyaner D, Hardy WB, Moorman MA, McIntosh KR, Mosca JD. Characterization and functionality of cell surface molecules on human mesenchymal stem cells. J Biomed. Sci 2003;10:228–241. [PubMed: 12595759]

Makino S, Fukuda K, Miyoshi S, Konishi F, Kodama H, Pan J, Sano M, Takahashi T, Hori S, Abe H, Hata J, Umezawa A, Ogawa S. Cardiomyocytes can be generated from marrow stromal cells in vitro. J. Clin. Invest 1999;103:697–705. [PubMed: 10074487]

Martin FT, Dwyer RM, Kelly J, Khan S, Murphy JM, Curran C, Miller N, Hennessy E, Dockery P, Barry FP, O'Brien T, Kerin MJ. Potential role of mesenchymal stem cells (MSCs) in the breast tumour microenvironment: stimulation of epithelial to mesenchymal transition (EMT). Breast Cancer Res. Treat. 2010

McCormick RJ, Musch TI, Bergman BC, Thomas DP. Regional differences in LV collagen accumulation and mature cross-linking after myocardial infarction in rats. Am. J. Physiol 1994;266:H354–H359. [PubMed: 8304518]

Nishiya D, Omura T, Shimada K, Matsumoto R, Kusuyama T, Enomoto S, Iwao H, Takeuchi K, Yoshikawa J, Yoshiyama M. Effects of erythropoietin on cardiac remodeling after myocardial infarction. J Pharmacol. Sci 2006;101:31–39. [PubMed: 16717399]

Piao H, Youn TJ, Kwon JS, Kim YH, Bae JW, Bora S, Kim DW, Cho MC, Lee MM, Park YB. Effects of bone marrow derived mesenchymal stem cells transplantation in acutely infarcting myocardium. Eur. J. Heart Fail 2005;7:730–738. [PubMed: 16158494]

Ren J, Babcock SA, Li Q, Huff AF, Li SY, Doser TA. Aldehyde dehydrogenase-2 transgene ameliorates chronic alcohol ingestion-induced apoptosis in cerebral cortex. Toxicol. Lett 2009;187:149–156. [PubMed: 19429258]

Tang J, Xie Q, Pan G, Wang J, Wang M. Mesenchymal stem cells participate in angiogenesis and improve heart function in rat model of myocardial ischemia with reperfusion. Eur J Cardiothorac. Surg 2006;30:353–361. [PubMed: 16829080]

Toma C, Pittenger MF, Cahill KS, Byrne BJ, Kessler PD. Human mesenchymal stem cells differentiate to a cardiomyocyte phenotype in the adult murine heart. Circulation 2002;105:93–98. [PubMed: 11772882]

Tomita S, Li RK, Weisel RD, Mickle DA, Kim EJ, Sakai T, Jia ZQ. Autologous transplantation of bone marrow cells improves damaged heart function. Circulation 1999;100:II247–II256. [PubMed: 10567312]

Tomita Y, Makino S, Hakuno D, Hattan N, Kimura K, Miyoshi S, Murata M, Ieda M, Fukuda K. Application of mesenchymal stem cell-derived cardiomyocytes as bio-pacemakers: current status and problems to be solved. Med. Biol. Eng Comput 2007;45:209–220. [PubMed: 17262204]

Urbanek K, Torella D, Sheikh F, De AA, Nurzynska D, Silvestri F, Beltrami CA, Bussani R, Beltrami AP, Quaini F, Bolli R, Leri A, Kajstura J, Anversa P. Myocardial regeneration by activation of multipotent cardiac stem cells in ischemic heart failure. Proc. Natl. Acad. Sci. U. S. A 2005;102:8692–8697. [PubMed: 15932947]

Vertesaljai M, Piroth Z, Fontos G, Andreka G, Font G, Szantho G, Lueff S, Reti M, Masszi T, Ablonczy L, Juhasz ED, Simor T, Turner MS, Andreka P. Drugs, gene transfer, signaling factors: a bench to bedside approach to myocardial stem cell therapy. Heart Fail. Rev 2008;13:227–244. [PubMed: 17668319]

Wang YQ, Wang M, Zhang P, Song JJ, Li YP, Hou SH, Huang CX. Effect of transplanted mesenchymal stem cells from rats of different ages on the improvement of heart function after acute myocardial infarction. Chin Med. J. (Engl.) 2008;121:2290–2298. [PubMed: 19080335]

Yang X, Doser TA, Fang CX, Nunn JM, Janardhanan R, Zhu M, Sreejayan N, Quinn MT, Ren J. Metallothionein prolongs survival and antagonizes senescence-associated cardiomyocyte diastolic dysfunction: role of oxidative stress. FASEB J 2006;20:1024–1026. [PubMed: 16585059]

Zhang M, Methot D, Poppa V, Fujio Y, Walsh K, Murry CE. Cardiomyocyte grafting for cardiac repair: graft cell death and anti-death strategies. J Mol. Cell Cardiol 2001;33:907–921. [PubMed: 11343414]
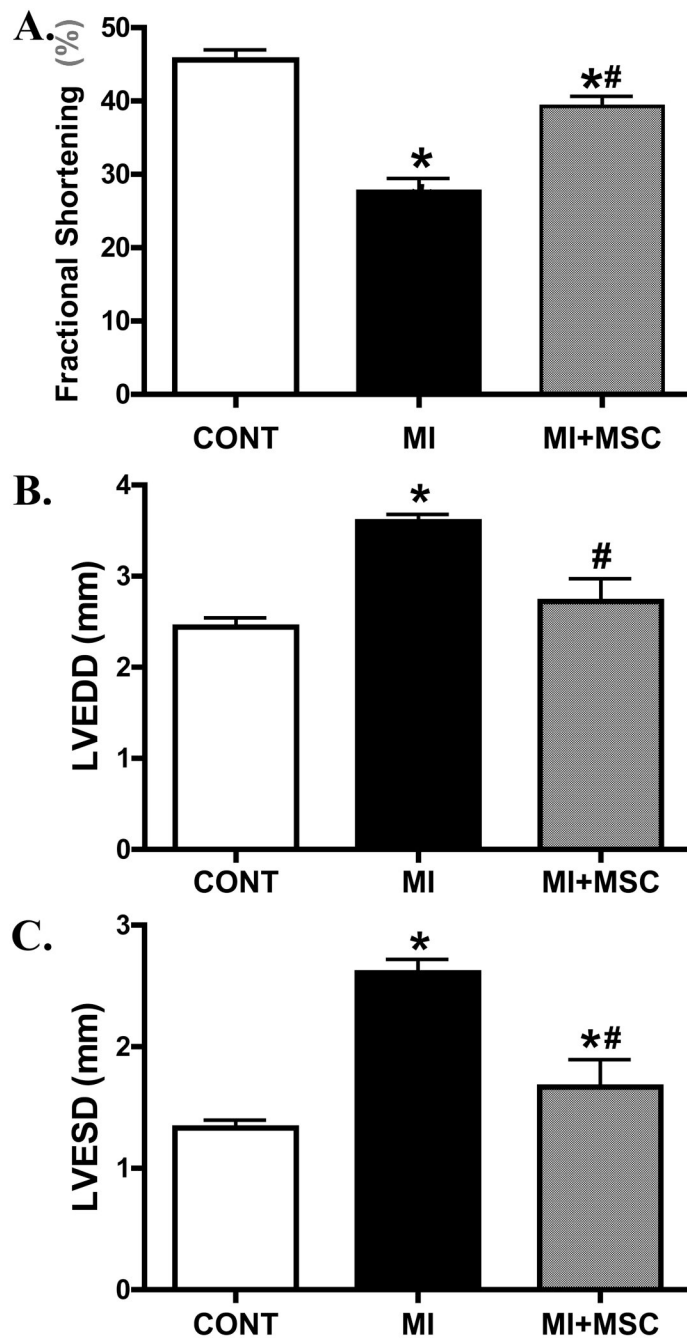
Fig. 1.
Echocardiographic evaluation of murine hearts following MI with or without MSC
transplantation. A: Fraction shortening (%); B: Left ventricular end diastolic diameter
(LVEDD); C: Left ventricular end systolic diameter (LVESD) Mean ± SEM, n = 5–7 mice per
group, * $p < 0.05$ *vs.* C57 control (CONT) group; # $p < 0.05$ *vs.* MI group.
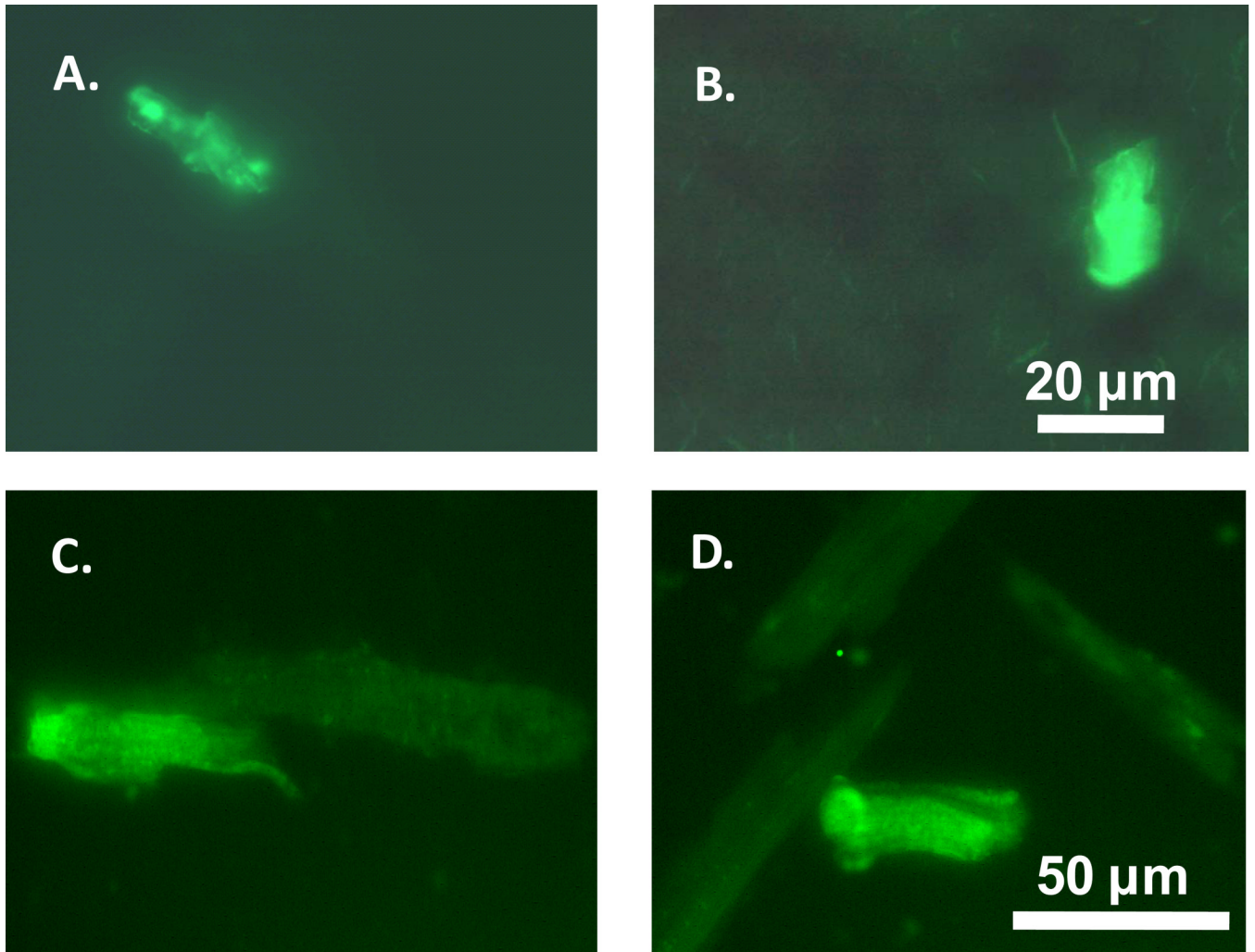
Fig. 2.
Illustration of the EGFP-positive cells from frozen heart slices or isolated myocytes from the MI border zones 10 days after the MSCs transplantation. A, B: heart tissues; C, D: isolated cardiomyocytes.
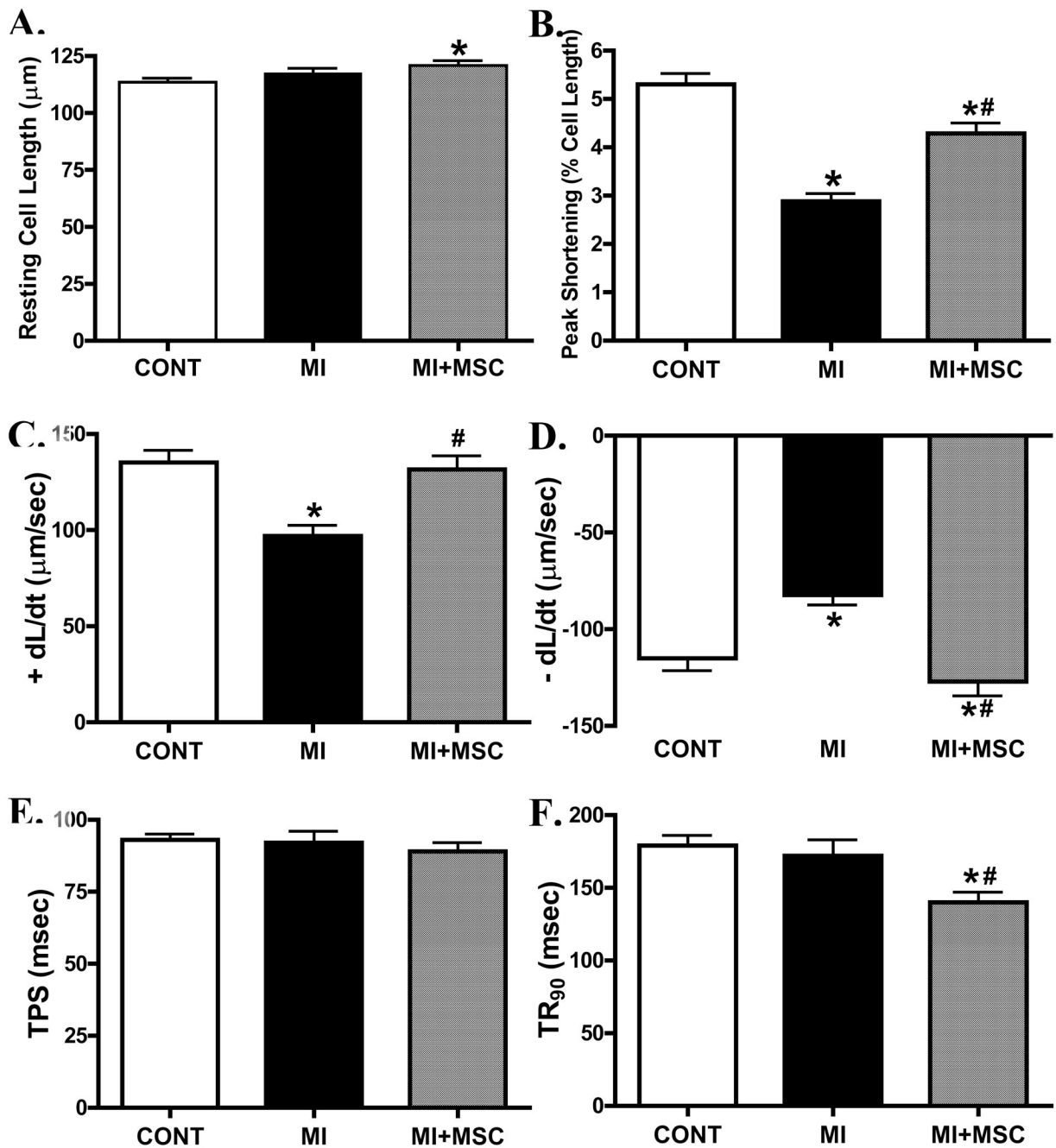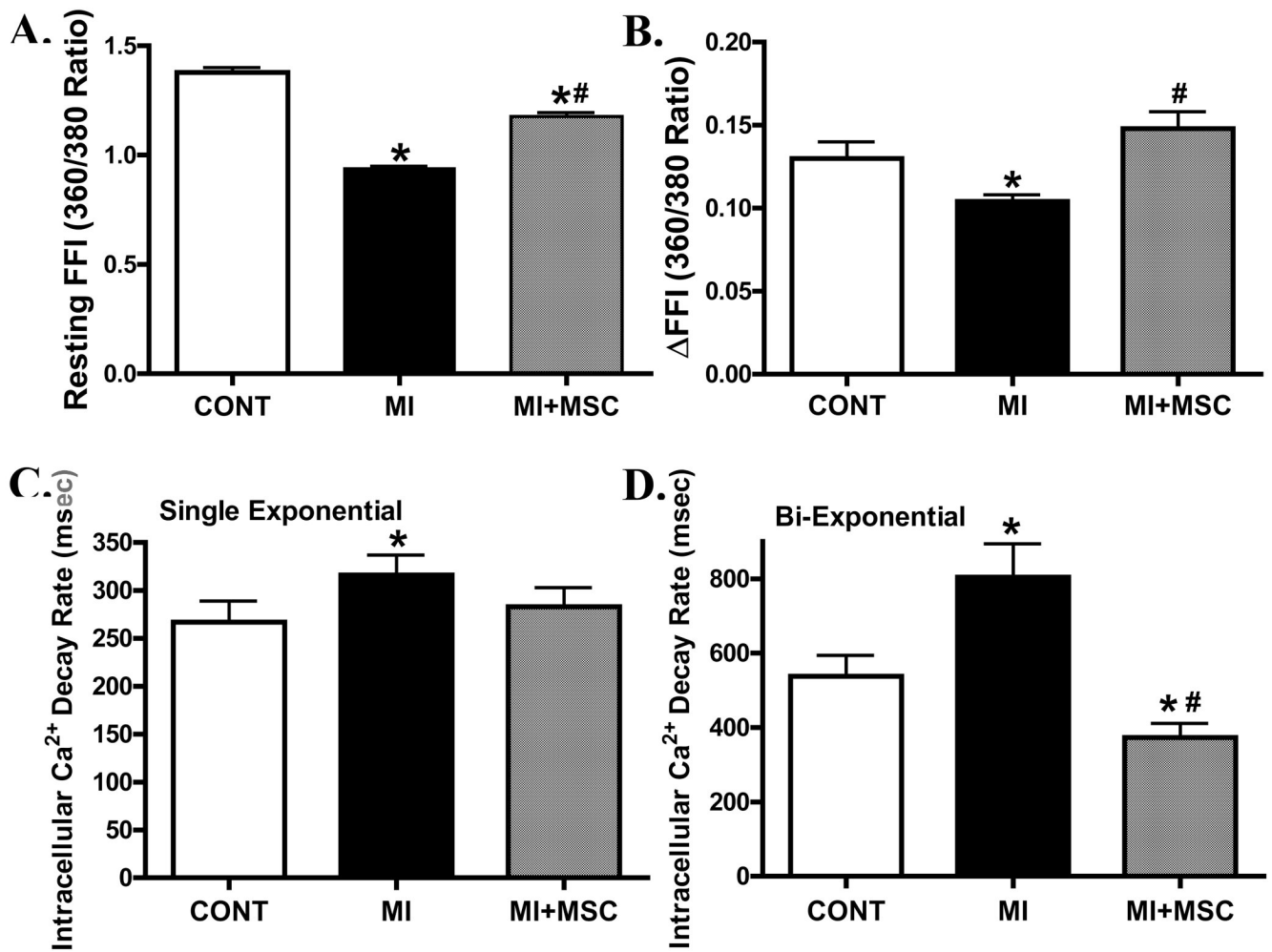
Fig. 3.
Effect of MI on cell shortening in cardiomyocytes from area at risk in the absence or presence of MSC transplantation. (A): resting cell length; (B): peak shortening (normalized to resting cell length); (C, D): maximal velocity of cell relengthening/shortening ($\pm$ dL/dt); (E): time-to-peak shortening (TPS); and (F): time-to-90% relengthening (TR$_{90}$). Mean $\pm$ SEM, n = 140–148 myocytes per group, * $p < 0.05$ *vs.* C57 control (CONT) group; # $p < 0.05$ *vs.* MI group.

Fig. 4.
Effect of MI on intracellular Ca^{2+} properties in cardiomyocytes from area at risk in the absence or presence of MSC transplantation. (A): Baseline intracellular Ca^{2+} fura-2 fluorescence intensity (FFI); (B): Electrically-stimulated increase in fura-2 fluorescence intensity (ΔFFI); (C): Single-exponential Ca^{2+} transient decay rate and (D): Bi-exponential Ca^{2+} transient decay rate. Mean ± SEM, n = 38–61 cells per group, * $p < 0.05$ *vs.* C57 control (CONT) group; # $p < 0.05$ *vs.* MI group.
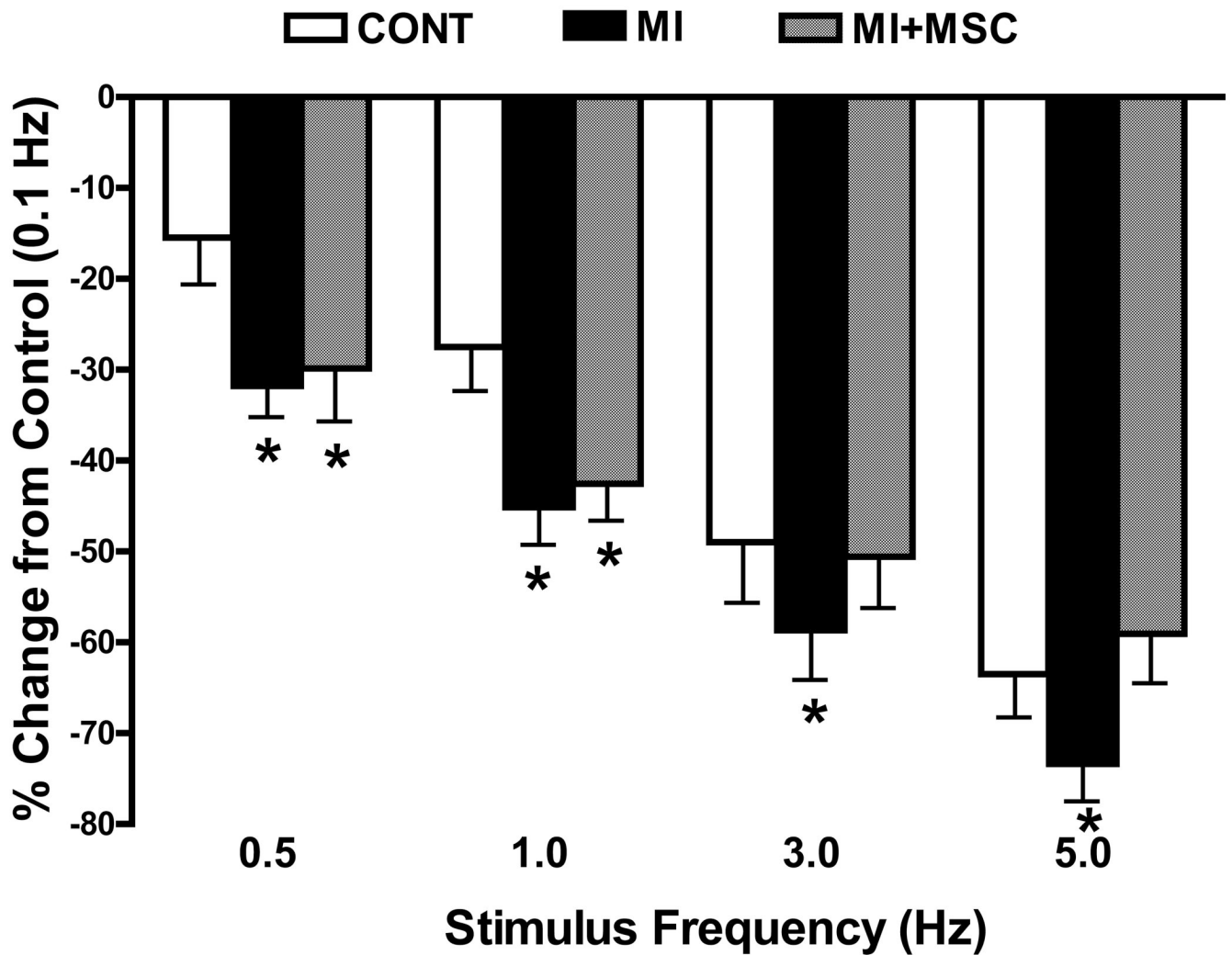
Fig. 5.
Change in peak shortening (PS) amplitude of cardiomyocytes from area at risk following MI in the absence or presence of MSC transplantation at different stimulus frequencies (0.1 – 5.0 Hz). PS at various stimulus frequencies was normalized to PS value obtained at 0.1 Hz from the same cell. Mean ± SEM, n = 22 cells per group, *p < 0.05 *vs.* control (CONT) group.
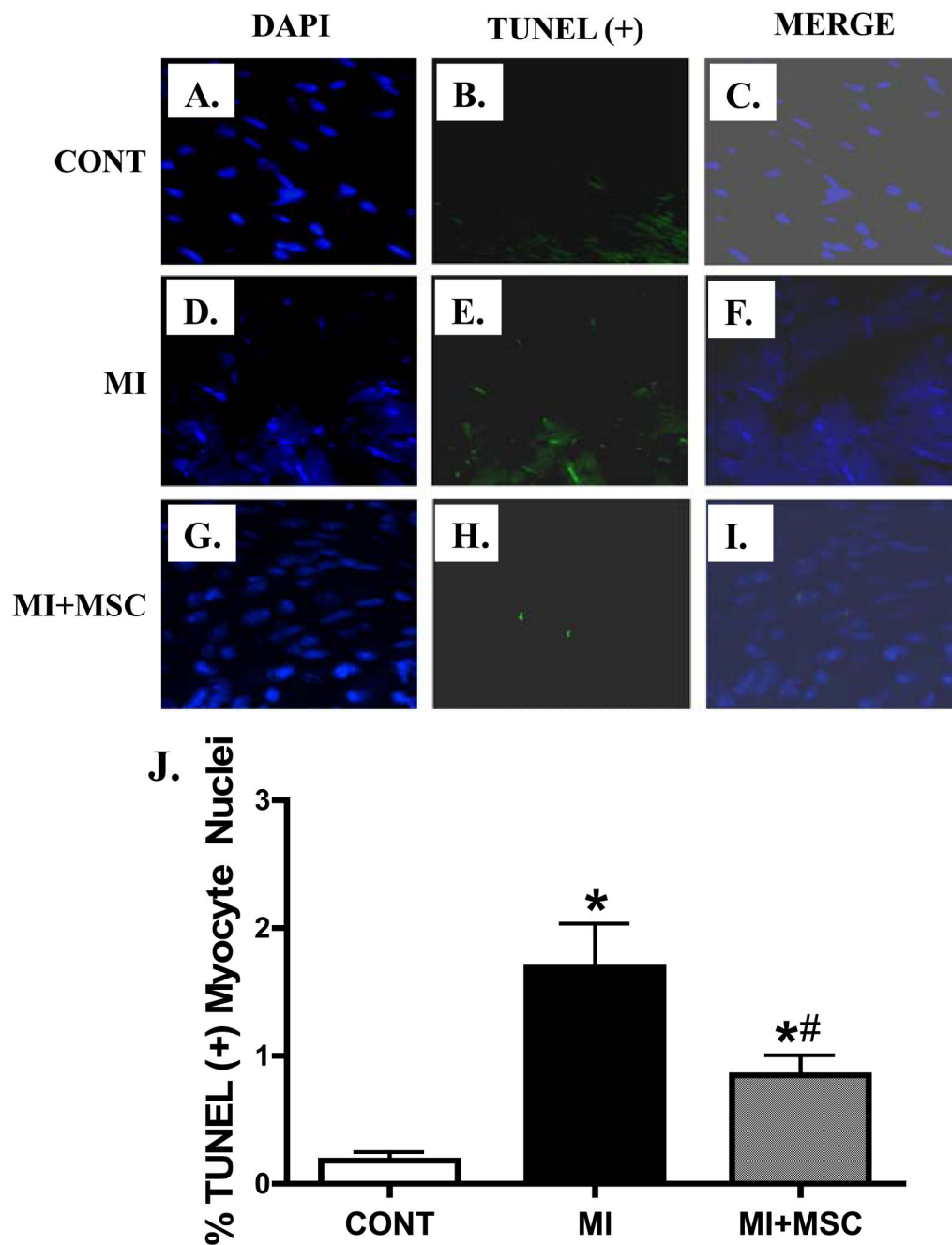
Fig. 6.
Effect of MI on apoptosis using TUNEL staining in myocardium from area at risk in the absence or presence of MSC transplantation. All nuclei were stained with DAPI shown in blue in panel A (Control), D (MI) and G (MI+MSC); TUNEL(+) nuclei were visualized with fluorescein (green) in panel B (Control), E (MI) and H (MI+MSC); Panels C (Control), F (MI) and I (MI+MSC) displayed merged DAPI and TUNEL (+) nuclei staining. Mean ± SEM, n = 21 – 30 fields from 3 mice per group, * p < 0.05 *vs.* control (CONT); # p < 0.05 *vs.* MI group.
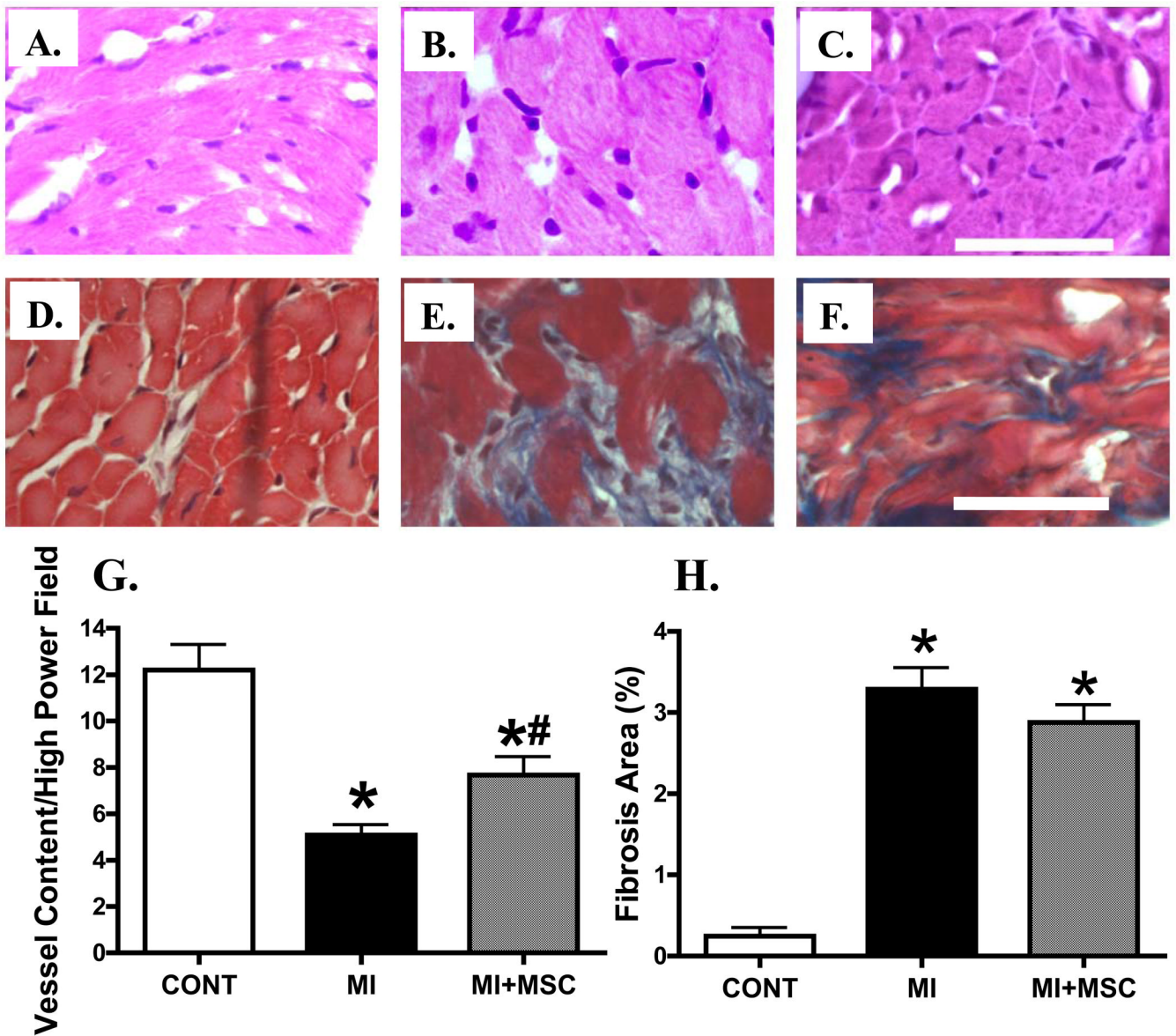
Fig. 7.
H&E and Masson trichrome stained photomicrographs exhibiting angiogenesis and myocardial fibrosis, respectively, in myocardium from area at risk in the absence or presence of MSC transplantation. Panels A (Control), B (MI) and C (MI+MSC) display H&E staining indicative of vascular content; Panels D (Control), E (MI) and F (MI+MSC) display Masson trichrome staining exhibiting myocardial fibrosis. Panels G and H depict pooled data of vessel content (H&E staining) and myocardial fibrosis (Mason trichrome), respectively. Scale bar = 50 μm. Mean ± SEM, n = 10 – 15 fields from 3 mice per group, * $p < 0.05$ *vs.* control (CONT), # $p < 0.05$ *vs.* MI group.